Charge Carrier Transport in Poly(*N*-vinylcarbazole):CdS Quantum Dot Hybrid Nanocomposite

Kaushik Roy Choudhury, Marek Samoc,† Amitava Patra,‡ and Paras N. Prasad*

Institute for Lasers, Photonics and Biophotonics, Departments of Physics and Chemistry, University at Buffalo, The State University of New York, Buffalo, New York 14260

Received: July 16, 2003; In Final Form: November 1, 2003

Hybrid organic:inorganic materials have emerged as a novel class of electronic and optoelectronic media for a number of potential technological applications. However, very little fundamental understanding of charge carrier transport in such hybrid materials exists. A knowledge of the influence of nanoparticle doping on charge carrier mobility in nano composites becomes important in order to optimize properties for photorefractive and photovoltaic operations. We report here a study of the mobility of holes in a model nanoparticle-sensitized hybrid organic:inorganic system consisting of poly(*N*-vinylcarbazole) (PVK) doped with quantum dots of cadmium sulfide. The mobility of holes (dominant carriers in the PVK host materials) was measured using the conventional time-of-flight technique with injection of holes from a selenium layer. Though photocurrent transients exhibit features typical of dispersive transport in an amorphous semiconductor, certain deviations from the original Scher-Montroll theory are observed. Strong dependence of the carrier mobility on field and temperature indicate Poole−Frenkel-like activated hopping transport. A thickness dependence stronger than that suggested by the Scher−Montroll theory is found. Significant enhancement of the effective carrier mobility is noticed with the increase of nanoparticle concentration, still well below the percolation limit. A simple theoretical model based on time- and mean-free-path dependent mobility is proposed to account for this surprising result, which provides a good fit to the experimental data obtained.

Introduction

In recent years, there has been a substantial rise in interest regarding the use of nanosize metal and semiconductor particles as components of various composite materials intended to possess fine-tuned electrical and optical properties.[1−9] The advantage of nanoparticles, as compared to more classical bulk homogeneous materials, is that they bridge a gap between the properties of these different classes of substances. On one hand, a nanoparticle may be regarded as a lump of bulk material and its properties may be derived by considering the spatial confinement imposed on electrons and excitations as a result of the particle's limited size. On the other hand, a nanoparticle can be thought of as a big molecule that can be functionalized (capped) and that can interact with its surroundings in a way similar to conventional molecules. Control over the properties[10−12] of nanoparticles can be exerted by modifying their composition (e.g., in the case of semiconductors one can often change their stoichiometry and tune the band gap), the size and shape of nanoparticles of a given composition, and their capping moiety. The tuning of the spectral properties of semiconductor nanocrystals, especially for CdS, is well-known.[11−15] The color of CdS nanocrystal quantum dots (QCdS) can be varied from the orange color of the bulk material to yellow and finally to white, in which case the optical band-gap has shifted to the ultra-violet region of the spectrum. This blue-shift in the optical band-gap is known as the quantum size effect[16−20] and is also accompanied by an increase in the absorption cross section. The size at which quantum confinement is observed varies from material to material depending on the value of the Bohr radius: the radius corresponding to the size of the exciton in the material. The tunability of the properties of nanoparticles achieved by controlling their composition, size, and interface with the matrix may provide an advantage in formulating new composite materials with optimized properties for various applications.[21,22] We are concerned here with the applications of nanoparticles as dopants in polymer-based composites that may be used as photoconductors (e.g., for photovoltaic applications), light emitting materials, or photorefractive media. In these applications, the nanoparticles may contribute to the different elementary steps of the electrical and optical processes occurring under illumination or under the application of an electrical field. Photoconductive polymer composites usually contain components with well-defined functions, although often a component may play more than a single role. For the case of PVK based photoconductors, the polymer provides for a structural matrix and serves as the hole-transporting agent.[14,23,24] Due to the lack of intrinsic absorption in the visible region associated with PVK, a photogeneration activating component must also be included. In the case of photorefractive materials, the refractive index of the composite can be effectively modulated through the inclusion of an electrooptic active component,[25,26] and in the case of electroluminescent materials, components enhancing the recombination of charge carriers and the electroluminescent light emission are included.[3] Semiconductor nanoparticles can, in principle, be used in multiple roles in such composites. Because the mobility of charge carriers in semiconductors is higher (and less dependent on the electric field) than in organics, the nanoparticles present at high concentration exceeding the

* To whom correspondence should be addressed. Fax: (716) 645-6945. Phone: (716) 645-6800 ext. 2099. E-mail: pnprasad@acsu.buffalo.edu.

† Permanent address: Laser Physics Centre, The Australian National University, Canberra, Australia.

‡ Permanent address: Sol-Gel Division, Central Glass & Ceramic Research Institute, Kolkata, India.

10.1021/jp0360671 CCC: $27.50
Published on Web 01/09/2004

percolation threshold are likely to provide improved charge transport through the network of the nanoparticles.[27,28] The quantum dot semiconductors may be effective photocharge generators due to the high efficiency of the primary photogeneration processes in semiconductors. Other roles are also possible. We concentrate here on the single aspect of the influence of nanoparticles on the transport of charge carriers in nanocomposites: the unipolar (one-carrier) transport through a polymer matrix with relatively low density of semiconductor quantum dots. Therefore, we separate here this influence from the photogeneration processes and the recombination processes occurring under the conditions of application of electric field and impingement of light on a nanocomposite. The fundamental question that we are attempting to address in this paper is whether the introduction of semiconductor nanoparticles into a polymer matrix causes any noticeable improvement or deterioration of carrier transport. Preliminary results of this study were communicated in ref 9.

A frequently cited limitation of polymeric photorefractive materials is their relatively slow response time which is generally limited by the charge-carrier mobility, μ. Thus, a knowledge of the influence of nanoparticle doping on charge transport in the composites becomes important for optimizing properties of such composites. Even among the molecularly doped polymeric photorefractive materials, few studies have been conducted characterizing the charge transport properties,[29] accentuating the need for such investigations. Despite the lack of direct time-of-flight mobility data, the problem has already been addressed by Wang and Herron,[30] who estimated the charge carrier mobilities from peak values of the space-charge limited photocurrents in a nanoparticle doped polymer. The conclusion was that the mobility of charge carriers is essentially unchanged compared to pure polymer. Here we report on more detailed transient photocurrent measurements performed to estimate the parameters characterizing the carrier transport. The system under investigation is that of poly(*N*-vinylcarbazole) (PVK), one of the most well characterized photoconductive polymers,[25,26,31−33] doped with nanoparticles of cadmium sulfide. This model system is important because it is similar to the QCdS sensitized photorefractive mixtures investigated by us before and found interesting because of their high efficiency of photogeneration at moderate electrical fields.[25,26] Indeed, in addition to the desirable spectral qualities associated with nanocrystal photosensitization, the ability to achieve a photocharge generation quantum efficiency in excess of that attributed to common organic dyes for a given electric field has also been demonstrated.[26]

Experimental Section

A. Nanocrystal Synthesis. Various chemical methods have been developed to control the size and distribution of nanoparticles during synthesis. Due to the high surface area and the surface energy, the nanoparticles undergo aggregation into larger particles. In conventional methods, uncontrolled nucleation and subsequent growth of the precipitated particles in a bulk aqueous medium finally generates larger particles with a wide size distribution. To overcome these problems, many recent studies have used emulsions[34−37] to control the size and morphology of the nanoparticles. Generally, the reverse micelles formed in water-in-oil (w/o) type emulsions act as micro- or nanoreactors in which reactions are carried out.[36,37] In practice, the "water phase" having a high dielectric constant is dispersed under agitation into an "oil phase" (water-immiscible organic solvent), having a low dielectric constant. It is known that a minimum critical micelle concentration (CMC) is needed for the surfactant molecules to self-aggregate, giving rise to "reverse micelles" in organic solvents.

The starting materials for CdS preparation were cadmium acetate and sodium sulfide. Aqueous solutions of cadmium acetate (of varying concentration) and sodium sulfide were prepared by dissolving the respective salts in deionized water. The support solvent containing 5 vol % of Span 80 in cyclohexane was used for emulsification, i.e., for the preparation of w/o emulsion in the present study. The cadmium acetate solution was dispersed in a measured volume of the support solvent under mechanical agitation to obtain a w/o emulsion. The required amount of sodium sulfide solution was then added slowly to the support solvent under mechanical agitation. The stabilized emulsion was then subjected to an ultrasonic treatment at 26 kHz for 10 min and was stirred for 10 min. The CdS particles were collected from the reverse micellar solutions by adding a known volume of methanol. Immediate separation of particles occurred. The particles were collected using centrifugation at 6000 rpm. To remove the last traces of adhered impurities, the particles were washed twice with methanol and then with acetone, each time the particles being collected by centrifugation as described above. The washed particles were dried at 60 °C overnight. By varying the aging time and by changing the cadmium salt concentration, we can exercise a degree of control over the ultimate size of the resulting nanocrystals (NCs). In this case, the NCs were permitted to grow until the band gap coincided with the wavelength of radiation used in this study.

The morphology of the powder was examined using transmission electron microscopy (TEM). Crystal phases were identified using X-ray diffractometry (XRD) using nickel-filtered Cu Kα radiation. The crystallite sizes of the nanoparticles were calculated following the Scherrer's equation

$$D = K\lambda/\beta \cos\theta \qquad (1)$$

where $K = 0.9$, D represents crystallite size (A), λ is the wavelength of Cu Kα radiation, and β the corrected half width of the diffraction peak.

The estimated average crystal sizes (from TEM picture) are $\sim$10 nm at 60 °C heat-treated samples.

B. Measurements. In the sample fabrication process, first a charge-generating layer of selenium (<1 μm) is deposited by high vacuum deposition onto commercially acquired glass substrates precoated with indium tin oxide (Thin Film Devices). The QCdS was dispersed in pyridine by sonication and PVK (secondary standard, purchased from Aldrich) was subsequently dissolved in it by mechanical agitation. The solution was then spun onto the selenium coated ITO-glass substrate. A dynamic vacuum condition served to remove the pyridine encapsulating the QCdS and thus creating a direct interface between the quantum dot and the polymer matrix. Because capping of a nanoparticle may influence its capability of exchanging charges with the matrix, the efficiency of this procedure may be important; however, we have not detected changes in the mobility between samples that were vacuum treated for a different time. The thickness of the films, as determined by an Alpha step profiler, ranged between 2.5 and 9 μm. Subsequently, silver counter electrodes (area $\sim$0.4 cm^2) were fabricated by high vacuum deposition to form a sandwich device structure.

The mobility of holes (dominant carriers in the PVK host materials) was measured using the conventional time-of-flight technique[38] (Figure 1). Impurities contained within even carefully purified PVK inhibit the effective electron mobility within

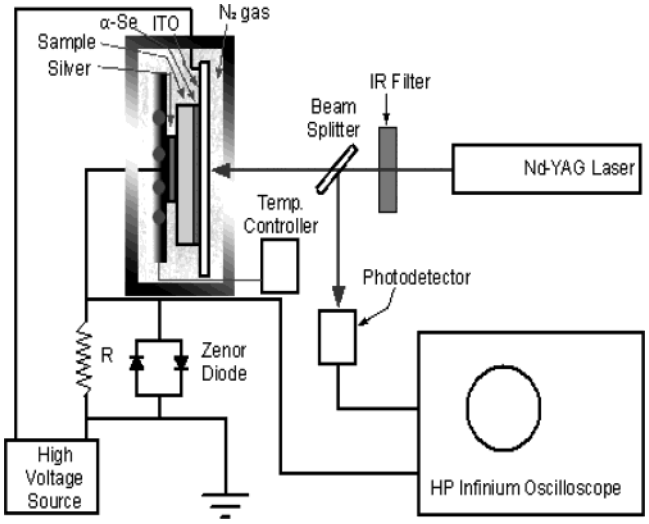

Figure 1. Experimental setup employed for the time-of-flight mobility measurements.

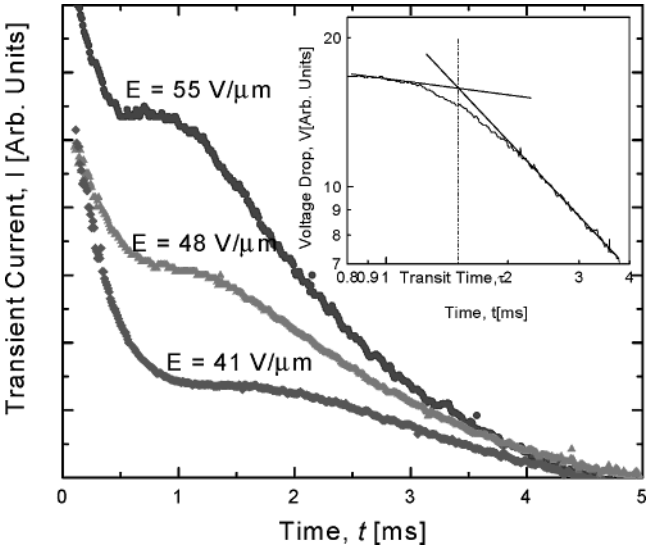

Figure 2. Current transient curves for a 2% CdS:PVK sample of 3.5 μm thickness at 297 K. The inset shows a typical trace on a log I vs log t plot used to determine transit time.

this matrix due to very strong trapping as was observed for this composite. An Nd:YAG laser operating at 532 nm with 10 ns pulses was used to irradiate the sample from the ITO side. Efficient photoinjection of holes occurring at the Se/PVK interface led to the appearance of hole transients attributable to transport in the polymer layer under the influence of applied bias. The current was detected by an external circuitry as shown in Figure 1 and recorded on a digital oscilloscope. Most transients were measured using relatively high-intensity light pulses, because transit times were better defined under space-charge-limited conditions. For temperature-dependent studies, the sample was mounted on a thermal block whose temperature could be controlled to 1 °C.

Results of Time-of-Flight Measurements and Discussion

The time-of flight technique of investigating charge carrier transport in photoconductors has been extensively used to determine the charge carrier mobilities in polymeric materials.[39−43] These studies were especially important because of the use of polymers of poly-*N*-vinylcarbazole type as active media in electrophotography. Our study of nanoparticle doped PVK must naturally refer to analogous studies on undoped PVK and on PVK doped with various additives. A confusing issue in these studies is the degree to which the charge carrier transport can be considered to be dispersive, as in the well-known Scher−Montroll theory[44] and whether the doping leads to less or more localization of charge carriers and, in effect, to increase or decrease of the effective mobility. The term "effective" mobility is necessary because, in most materials of similar composition, the mobility is not a constant, but a quantity that is electric field dependent and sample thickness dependent.[45,46]

The usual criterion for invoking dispersive transport models is the presence of a wide distribution of times of arrival of carriers at the counter electrode (as evidenced by a long "tail" in the current transient) and "universality" of the current transients obtained at different bias voltages and for different samples. The current transients obtained in our measurements exhibit characteristically pronounced "tails" (see Figure 2 for an example) and therefore the interpretation of transport in terms of the Scher−Montroll theory is an obvious choice. However, one needs to be careful in this interpretation because the experiments have been performed under conditions that are not entirely in agreement with simplified models. We recall that the classical "Scher−Montroll" shape of a current transient is a curve that presents two straight-line sections in double log coordinates. The section before the transit time t_f can be approximated by the power law: $I = \text{const}\ t^{-1+\alpha}$ and the section after the transit time is approximated by another power law: $I = \text{const}\ t^{-1-\alpha}$. Thus, a simple check of the applicability of the Scher−Montroll model is that the sum of the two exponents should be −2. However, it is apparent that such a relation does not hold strictly for the transients presented in Figure 2. Moreover, the portions of the transients before the apparent transit time are not well approximated by the power law. One reason for this discrepancy is obviously the fact that the measurements have been performed under the conditions that cannot be approximated as "small signal". We recall here that a "small signal approximation" means that the amount of excess charge photogenerated or photoinjected into the sample under investigation is so small that the electric field within the sample is not noticeably disturbed and can still be considered constant, given by $F = V/L \neq F(x)$. In other words, if the charge can be considered injected in a thin sheet, at $t = 0$ the maximum injected charge density $\rho(x) = \rho_0\delta(x - 0)$ is such that the field collapses to zero at the injection plane $x = 0$. Thus, Poisson's equation gives $F(x)_{x>0} = V/L$ and $\rho_0 = \epsilon\epsilon_0 V/L$. Under these space-charge perturbed conditions the average field acting on the carriers at $t = 0$ is $V/2L$. As the carriers move toward the counter electrode, the average field acting on them, and, especially the field acting on the fastest carriers will increase.

Even in the case of field-independent trap-free charge carrier mobility the presence of space-charge effects will lead to three effects: (1) broadening of the sheet of traveling charge carriers because of the different fields acting on the front of the carrier distribution and on its tail; (2) increase of the current as the function of time for the times shorter than that of arrival of the fastest carriers at the counter electrode; (3) shortening of the transit time compared to that for the small signal case.

These features have been recognized as early as in the sixties following Many et al.,[47] who considered a space-charge transient under the conditions of a step voltage applied to a system with an ohmic (i.e., injecting) electrode. Relatively little work has been done to understand how space-charge effects influence current transients under the conditions of the presence of dispersive transport. Qualitative description of these effects can,

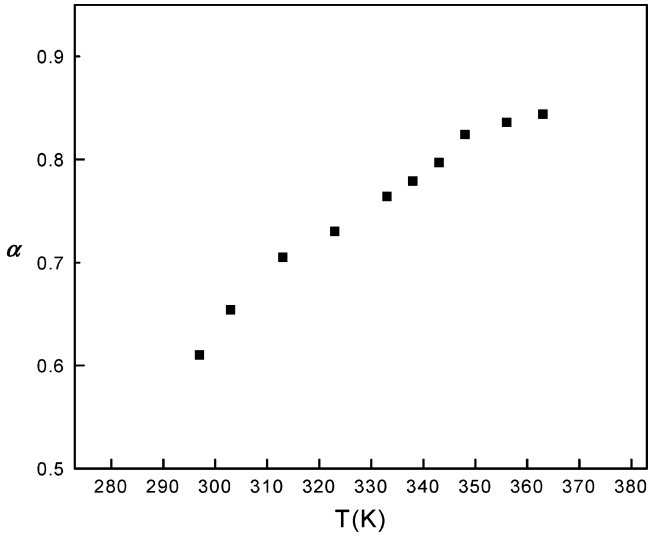

Figure 3. Variation of the dispersivity parameter α with temperature for a typical nanoparticle doped sample.

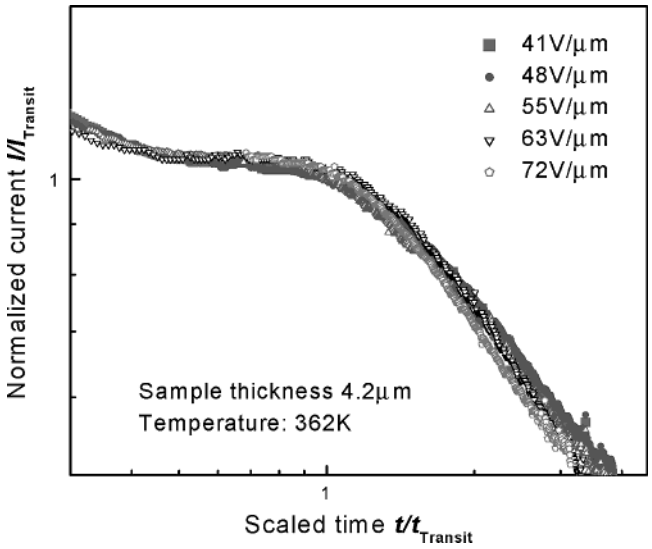

Figure 4. "Universal" curve obtained by superimposing several transients obtained for a sample of nanoparticle doped PVK at several voltages.

however, be attempted on the basis of numerical simulations[48] and simple considerations.

The original Scher−Montroll theory operates in the small signal approximation; thus, the electric field is considered constant and the drift velocity of carriers is considered to decrease in time because of the waiting time distribution $\psi(t) \propto t^{-\alpha}$, leading to a time-dependent mobility. Superposition of this behavior with that due to space−charge effects is going to lead to the following:

(1) "flattening" of the part of the transient before the apparent transit time: due to the fastest carriers moving gradually into higher and higher field and also due to the fact the mobility of charge carriers may be intrinsically field dependent, leading to even more prominent speeding up of the fastest carriers

(2) additional broadening of the distribution of arrival times of the carriers at the counter electrode due to the effect of slowing down the carriers that are left close to the injecting electrode and thus remain in lower electric field.

Therefore, the α values derived from transients obtained under space−charge conditions cannot be considered reliable and by themselves cannot be taken as a proof or disproof of the presence

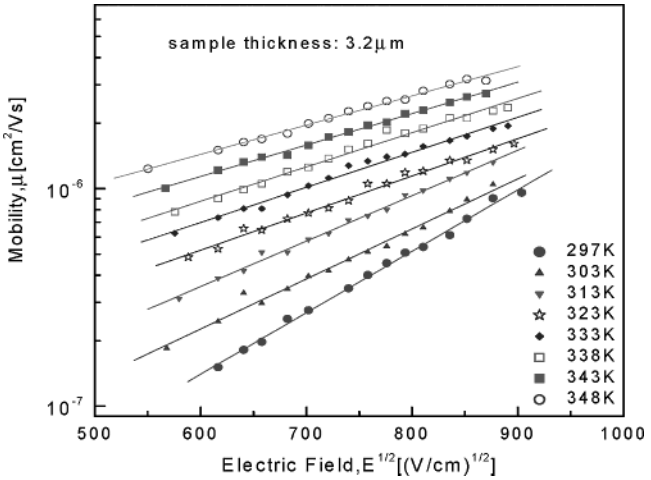

Figure 5. Gill formula presentation of the field dependences of the effective mobility in 2% nanoparticle doped PVK parametric in temperature: the Poole−Frenkel behavior.

of dispersive transport. Figure 3 shows values of α determined as a function of temperature. The trend of increasing α with temperature indicates that the transport becomes less dispersive at higher temperatures.

An argument can also be made regarding the "universality" of current transients. Figure 4 shows the superposition of several traces obtained for one of the samples investigated here. Although transients do look similar, there is certainly a trend causing the slopes of the lines to vary in such a way that a higher voltage makes the transient look less dispersive than the one at a lower voltage. This may be taken as an indication that the Scher−Montroll description is not strictly valid, but in view of the space-charge effects discussed above, some of the features of the transients may also be considered an artifact of the measurement.

Even before the introduction of the Scher-Montroll model, there have been numerous determinations of charge carrier mobility in PVK-like materials and the data obtained have been usually interpreted in terms of an empirical field and temperature dependence introduced by Gill.[31] The expression

$$\mu(E,T) = \mu_0 \exp\left(-\frac{\Delta_0 - \beta\sqrt{E}}{k_B T_{\text{eff}}}\right), \quad \text{where } \frac{1}{T_{\text{eff}}} = \frac{1}{T} - \frac{1}{T_0} \quad (2)$$

describes these dependences quite well and has been often taken as a proof of the Poole-Frenkel type activated hopping transport. Results of our experiments can also be relatively well fitted with the above formula as shown in Figures 5 and 6. The parameters in the above equation ($\Delta_0 = 0.46$ eV, $\mu_0 = 1.08 \times 10^{-5}$ cm²/Vs, $T_0 = 426$ K) are in a range similar to those for other PVK based systems. The Gill formula does not, however, predict the dependence of the charge carrier mobility on sample thickness. In fact, to obtain the dependences shown in Figures 5 and 6, it was necessary to perform all measurements on the same sample. The differences between the mobility values obtained for samples of the same composition but different thicknesses were much too big for results to overlap. Figure 7 shows the dependence of the charge carrier mobilities on the thickness. It is evident that the mobilities appear to be higher for thinner samples. This may be taken as another proof of the appropriateness of treating the mobility in terms of the dispersive transport models. One should, however, be aware that the thickness dependence seen in Figure 7 is, in fact, stronger than that predicted on the basis of the well-known formula derived

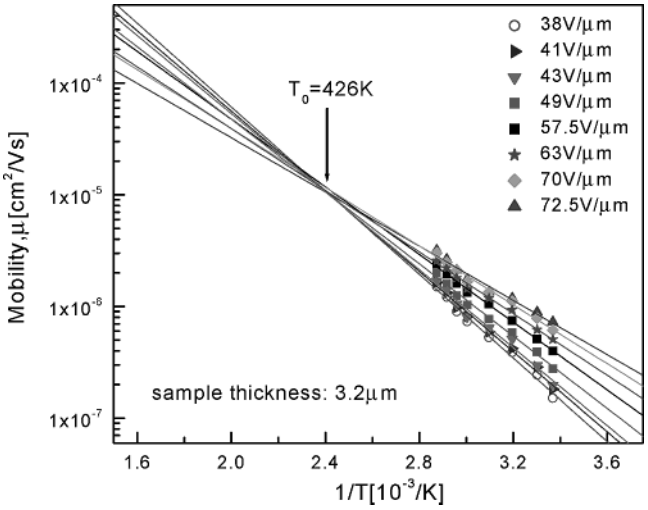

Figure 6. Temperature dependence of hole mobility parametric in electric field plotted on an ln μ vs T^{-1} scale: the Arrhenius behavior.

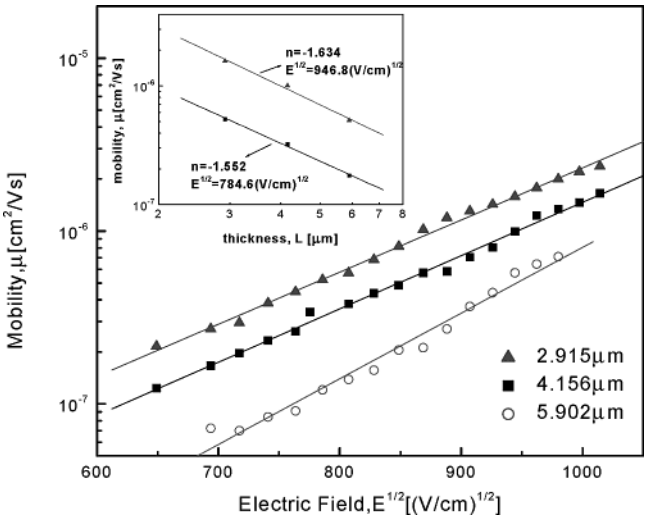

Figure 7. Comparison of the field dependences of hole mobilities in 2% CdS samples having varying thicknesses. Inset shows the variation of mobility with sample thickness for two different applied fields. The obtained slopes are −1.55 and −1.63 that correspond closely with the slope of −1.5 used for the theoretical fit in Figure 10.

from the Scher−Montroll theory, $\mu \propto L^{(\alpha-1)/\alpha}$. Several explanations of this feature can be offered. One can argue that the α values derived from the current transients are considerably altered by the space-charge effects and therefore the thickness dependence may be stronger than expected (i.e., the transport is indeed more dispersive than what might be expected on the basis of the current transients). Another possibility might be that the average field inside the samples is modified from the assumed value of V/L to a degree that is different for different thickness samples. It is also not impossible that the physical structure of samples of different thicknesses differs to a certain degree. These factors can alter the quantitative behavior of the $\mu(E)$ dependence, but the qualitative trends are as expected in all samples having different content of nanoparticles.

The most important result obtained in these mobility measurements is that shown in Figure 8 which represents the $\mu(E)$ dependence on nanoparticle concentrations. The immediate conclusion from these results is that the presence of nanoparticles does not impair in any way the charge carrier transport, but rather enhances the hole mobility. The degree of enhancement is certainly beyond the experimental error and thus one should ask why the effect is observed at all. This issue is discussed below.

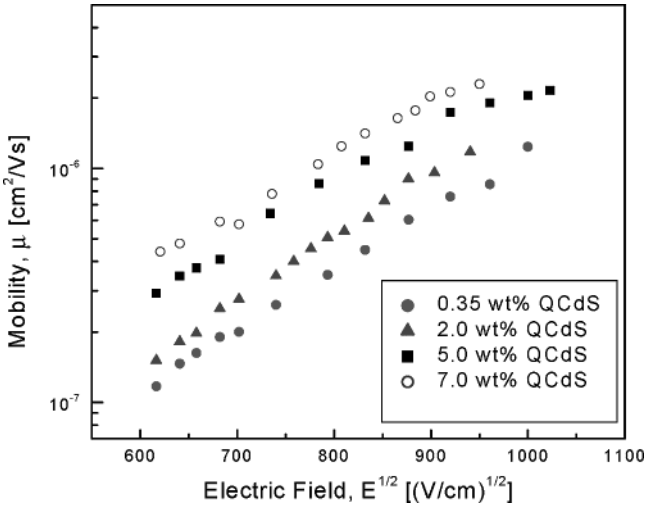

Figure 8. Comparison of field dependences of hole mobilities in samples of same thicknesses (3.2μm) having varying concentrations of CdS nanoparticles.

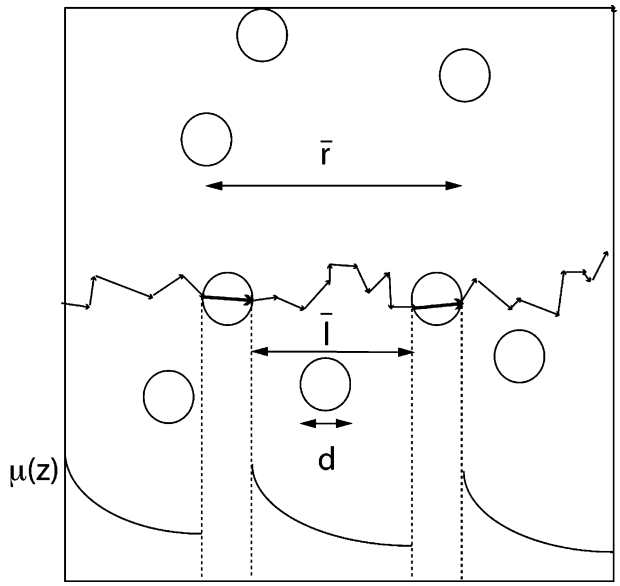

Figure 9. Scheme of transport of charge carriers through the nanocomposite.

Enhancement of Hole Mobility in Nanoparticle Doped Polymer. To discuss possible mechanisms of the influence of nanoparticles on the charge carrier transport in the composite material one needs to define and characterize some parameters describing such a material (Figure 9). The composites can be characterized by two parameters: the average diameter of the nanoparticles d and the volume fraction of nanoparticles x (which is related to the mass fraction g as $x = g/\rho_n/[g/\rho_n + (1 - g)/\rho_p]$ where ρ_n and ρ_p are densities of the nanoparticles and the polymer. In our case $\rho_n = 4.8$ g/cm^3 and $\rho_p = 1.2$ g/cm^3, therefore, e.g., 7 wt % of nanoparticles corresponds to $x = 0.017$). The concentration of the nanoparticles is thus $N = 6x/\pi d^3$. The average distance between the centers of nanoparticles can be approximated as $\bar{r} = N^{-1/3} = d(\pi/6x)^{1/3}$. With random distribution of nanoparticles within the matrix one can expect that percolation may occur when the distance between the nanoparticles becomes comparable with their diameters, i.e., $(\bar{r} - d)/d < 1$. Obviously, the concentrations used by us in the present study do not fulfill this criterion; thus, ordinary

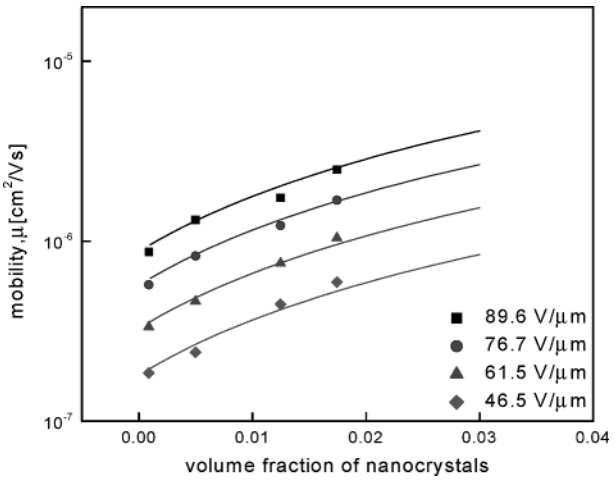

Figure 10. Dependence of the hole mobility on varying concentration of nanoparticles at four different applied electric fields. The solid lines are theoretical fits to the data.

percolation is not present. There have been reports about transport enhancement in heterogeneous systems where the highly conducting dopant forms well-defined paths of easy conduction by "reticulate doping".[49] Under such circumstances, the enhanced transport can take place at very low concentrations of the dopant. However, we do not have any indication that a similar situation may be present in our samples and that the distribution of the nanoparticles is not random.

The situation is also quite different from that of molecularly doped polymers[27] where the dopants are essentially uniformly distributed in the matrix of the polymer, and because of the small size of the dopant molecules, the average distance between them is so small that hops between the dopant molecules are possible. Thus, we need to assume that the transport in our samples proceeds mostly through the matrix of the polymer and is only modified to a certain extent by the nanoparticles. As mentioned before, there must be a concern about the possibility that the interface between the nanoparticle and the matrix may be of importance. In fact, it is known that transfer of a charge carrier from a nanoparticle into the surrounding matrix may be substantially hampered by the presence of a capping layer on the surface of the nanoparticle. The present results do not indicate that this is a problem in our samples. If blocking layers prevented the access to and from the nanoparticles, one would expect a reduction in the carrier mobility rather than an increase. The observed increase suggests direct participation of the nanoparticles in the conduction process.

We address now the magnitude of the relative enhancement of the mobility. In the simplest approximation one might think that a composite containing a volume fraction x of a high mobility (μ_n) component in a low mobility (μ_p) matrix should have a mobility that is a weighted average of the component mobilities, i.e., $1/\mu = x/\mu_n + (1 - x)/\mu_p$. This would, however, only increase the composite mobility by a factor $1/(1 - x)$ at the best, whereas we determine an enhancement by a factor of 3 to four in a 7 wt % (~1.7 vol %) composite.

To explain the enhancement of the mobility, we assume that the nanoparticles modify the dispersive transport in the matrix. In fact, the assumption that the process is dispersive is central to our explanation. We recall that the difference between the nondispersive hopping and dispersive hopping as discussed by Scher and Montroll is in the character of the hopping time distribution function $\psi(t)$. An exponential function would indicate nondispersive transport whereas a power function of the form $\psi(t) \sim t^{-(1+\alpha)}$ (where $0 < \alpha < 1$) is indicative of strong dispersion. The difference between these two cases is that the exponential waiting time distribution function does not change over the time elapsed, leading to time-independent average mobility, whereas the power function leads to a mobility that is time dependent: slowing down as the time elapses. The time-dependent mobility calls also for the thickness dependence of this parameter. These two dependences are often discussed in terms of Markoffian and non-Markoffian processes: that is processes that do not or do depend on the previous history. It appears from our data that encounters of charge carriers with nanoparticles do not lead to the increase of the transit time but shorten the time needed for the carriers to reach the counter electrode. Intuitively, such a situation might be possible if the nanoparticles act as extended trapping regions that compete with native traps. With the cross-section of an individual nanoparticle, σ_n, equal to $\pi d^2/4$ the mean free path of a carrier between encountering nanoparticles can be estimated as $\bar{l} = 1/N\sigma_n = 2d/3x$. As an example, for 15 nm particles present at a volume fraction of 0.01, this would amount to 1000 nm. Thus, the influence of nanoparticles on transport in films typically a few micrometers thick can be expected.

This behavior is modeled assuming the encounter of a carrier with a nanoparticle results in the loss of the "memory" that a carrier possesses in dispersive (non-Markoffian) transport. A nanoparticle of 10 nm diameter placed in a field of the order of 50 V/μm (as typical in our measurements) will have a potential difference as large as 0.5 V between its front and back. Therefore, considerable acceleration of a carrier is possible due to the mobility of holes in the semiconductor being much higher that that of the polymer matrix. At present, it is difficult to determine what degree of scattering will be present in CdS nanoparticles (that is to what degree the movement of the carrier inside the nanoparticle can be of ballistic character), but it is likely that at least some of the carriers may be ejected from nanoparticles with sufficient initial velocity to be considered entering the dispersive transport anew. This is illustrated in Figure 8. Figure 9 shows a comparison of the experimental dependences of the effective mobility on the concentration of nanoparticles with a simplistic model in which the mobility in a composite is calculated as an "effective mean-free-path" dependent quantity. In the spirit of the Scher-Montroll theory (and also multiple trapping models which lead essentially to the same result), we take the effective mobility as $\mu = \mu_0\langle L\rangle^n$ where the effective mean free path $\langle L\rangle$ is calculated as the geometrical average of a sample dependent thickness parameter L_0 and the mean free path of a carrier between encountering nanoparticles $\langle L\rangle^{-1} = L_0^{-1} + \bar{l}^{-1}$ where $\bar{l} = 1/N\sigma_n = 2d/3x$. It can be seen that, despite the conceptual simplicity of the above treatment, the agreement between the model and the experimental results is quite good. For the results plotted in Figure 9, the fit parameters are $n = -1.5$ and $L_0 = 0.7$ μm. Clearly, the best-fit L_0 appears to be smaller than the geometrical sample thickness, which may be due to oversimplification of the description of the actual microscopic transport process in the present model. Nevertheless, we feel that at least semiquantitatively we are able to account for the observed phenomena by invoking time- and mean-free-path-dependent mobility. We also find that the value of the power exponent n needed to fit the experimental dependence of the mobility on concentration is very similar to that describing the thickness dependence in Figure 7 (inset).

Conclusions

We have shown here that photoconductive composites obtained by doping of a host polymer with semiconductor

nanoparticles exhibit not only an increase of the photoconductivity due to sensitization of photocharge generation but the presence of nanoparticles may also lead to distinct increase of the effective mobility of charge carriers. A preliminary explanation of this phenomenon assumes an active role by the nanoparticles in the transport. The magnitude of enhancement is found to be consistent with a model invoking an effective mean free path-dependent mobility.

Acknowledgment. This research was supported in part by a Defense University Research Initiative on Nanotechnology (DURINT), Contract No. F496200110358, through the Directorate of Chemistry and Life Sciences of the Air Force Office of Scientific Research and in part by a NSF, DMR Solid State and Polymer Chemistry Grant No. DMR0075867. The authors thank Dr. Jeffrey Winiarz and Mr. Seongjin Jang for their active help in different stages of the study.

References and Notes

(1) Schlamp, M. C.; Peng, X.; Alivisatos, A. P. *J. Appl. Phys.* **1997**, *82*, 5837.
(2) Mattoussi, H.; Radzilowski, L. H.; Dabbousi, B. O.; Thomas, E. L.; Bawendi, M. G.; Rubner, M. F. *J. Appl. Phys*. **1998**, *83*, 7965.
(3) Coe, S.; Woo, W. K.; Bawendi, M.; Bulovic', V. *Science* **2002**, *420*, 800.
(4) Kagan, C. R.; Mitzi, D. B.; Dimitrakopoulos, C. D. *Science* **1999**, *286*, 945.
(5) Huynh, W. U.; Dittmer, J. J.; Alivisatos, A. P. *Science* **2002,** *295*, 2425.
(6) Wang, Y.; Herron, N. *J. Lumin*. **1996**, *70***,** 48.
(7) Herron, N.; Thorn, D. L. *Adv. Mater.* **1998**, *10***,** 1173.
(8) Lal, M.; Joshi, M.; Kumar, D. N.; Friend, C. S.; Winiarz, J.; Asefa, T.; Kim, K.; Prasad, P. N. *Mater. Res. Soc. Symp. Proc.* **1998**, *519***,** 217.
(9) Roy Choudhury, K.; Winiarz, J.; Samoc, M.; Prasad, P. N. *Appl. Phys. Lett.* **2003**, *82*, 406.
(10) Nirmal, M.; Brus, L. *Acc. Chem. Res.* **1999**, *32*, 407.
(11) Dabbousi, B. O.; Rodriguez-Viejo, J.; Mikulec, F. V.; Heine, J. R.; Mattoussi, H.; Ober, R.; Jensen, K. F.; Bawendi, M. G. *J. Phys. Chem. B* **1997**, *101*, 9463.
(12) Eychmiller, A. *J. Phys. Chem. B* **2000**, *104*, 6514.
(13) Trindade, T.; O'Brien, P.; Pickett, N. L. *Chem. Mater.* **2001**, *13*, 3843.
(14) Wang, S. H.; Yang, S. H.; Yang, C. L.; Li, Z. Q.; Wang, J. N.; Ge, W. K. *J. Phys. Chem. B* **2000**, *104*, 11853.
(15) Rossetti, R.; Hull, R.; Gibson, J. M.; Brus, L. E. *J. Chem. Phys.* **1985**, *82*, 552.
(16) Lee, J.; Tsakalakos, T. *Nanostruct. Mater.* **1997**, *8*, 381.
(17) Steigerwald, M. L.; Brus, L. E. *Acc. Chem. Res.* **1990**, *23*, 183.
(18) Nosaka, Y.; Ohta, N.; Miyama, H. *J. Phys. Chem.* **1990**, *94*, 3752.
(19) Wang, Y.; Herron, N. *J. Phys. Chem.* **1991**, *95*, 525.
(20) Wang, Y. In *Advances in Photochemistry*; Neckers, D. C., Volman, D. H., Von Bunau, G., Eds.; John Wiley and Sons: New York, 1995; Vol. 19.
(21) Herron, N.; Wang, Y. U.S. Patent 5,238,607, 1993.
(22) Wang, Y.; Herron, N. *Chem. Phys. Lett.* **1992**, *200*, 71.
(23) Shi, M. M.; Chen, H. Z.; Wang, M.; Ye, J. *Synth. Met.* **2003**, *137*, 1537.
(24) Cheng, J.; Wang, S.; Li, X.; Yan, Y.; Yang, S.; Yang, C. L.; Wang, J. N.; Ge, W. K. *Chem. Phys. Lett.* **2001**, *333*, 375.
(25) Winiarz, J. G.; Zhang, L.; Lal, M.; Friend, C. S.; Prasad, P. N. *J. Am. Chem. Soc.* **1999**, *121*, 5287.
(26) Winiarz, J. G.; Zhang, L.; Lal, M.; Friend, C. S.; Prasad, P. N. *Chem. Phys.* **1999**, *245*, 417.
(27) Dunlap, D. H. *Phys. Rev. B* **1995**, *52*, 939.
(28) Ambegaokar, V.; Halperin, B. I.; Langer, J. S. *Phys. Rev. B* **1971**, *4*, 2612.
(29) Hofmann, U.; Grasruck, M.; Leopold, A.; Schreiber, A.; Schloter, S.; Hohle, C.; Strohriegl, P.; Haarer, D.; Zilker, S. J. *J. Phys. Chem. B* **2000**, *104*, 3887.
(30) Wang, Y.; Herron, N. *J. Lumin.* **1996**, *70*, 48.
(31) Gill, W. D. *J. Appl. Phys.* **1972**, *43*, 5033.
(32) Pfister, G.; Griffiths, C. H. *Phys. Rev. Lett.* **1978**, *40*, 659.
(33) Bos, F. C.; Burland, D. M. *Phys. Rev. Lett.* **1987**, *58*, 152.
(34) Chatterjee, M.; Patra, A. *J. Am. Ceram. Soc.* **2001**, *84*, 1439.
(35) Chatterjee, M.; Naskar, M. K.; Siladitya, B.; Ganguli, D. *J. Mater. Res. Soc.* **2000**, *15*, 176.
(36) Masui, T.; Fujiwara, K.; Machida, K.; Adachi, G.; Sakata, T.; Mori, H. *Chem. Mater* **1997**, *9*, 2197.
(37) Lisiecki, I.; Bjorling, M.; Motte, L.; Ninham, B.; Pileni, M. P. *Langmuir* **1995**, *11*, 2385.
(38) Mort, J.; Pai, D. M. *Photoconductivity and Related Phenomena*; Elsevier Scientific: Amsterdam, 1976.
(39) Pfister, G. *Phys. Rev. B* **1977**, *16*, 3676.
(40) Im, C.; Bässler, H.; Rost, H.; Hörhold H. H. *J. Chem. Phys.* **2000**, *113*, 3802.
(41) Borsenberger, P. M.; Pautmeier, L.; Bässler H. *J. Chem. Phys.* **1991**, *94*, 5447.
(42) Blom, P. W. M.; Vissenberg, M. C. J. M. *Phys. Rev. Lett*. **1998**, *80*, 3819.
(43) Campbell, I. H.; Smith, D. L.; Neef, C. J.; Ferraris, J. P. *Appl. Phys. Lett.* **1999**, *74*, 2809.
(44) Schmidlin, F. W. *Phys. Rev. B* **1977**, *16*, 2362.
(45) Grasruck, M.; Schreiber, A.; Hofmann, U.; Zilker, S. J.; Leopold, A.; Schloter, S.; Hohle, C.; Strohriegl, P.; Haarer, D. *Phys. Rev. B* **1999**, *60*, 16543.
(46) Crisa, N. Phys. *Status Solidi B* **1983**, *116*, 269.
(47) Many, A.; Simhony, M.; Weisz S. Z.; Teucher Y. *J. Phys. Chem Sol.* **1964**, 25, 721.
(48) Chu, M. H.; Wu, C. H. J. Phys. Chem B **2000**, *104*, 3924.
(49) Jeszka, J. K.; Ulanski, J.; Kryszewski, M. *Nature* **1981**, *289*, 390.